



Cite this: *RSC Adv.*, 2021, 11, 3770

Received 1st December 2020  
Accepted 6th January 2021

DOI: 10.1039/d0ra10138a

rsc.li/rsc-advances

# Incorporation of *N*-phenyl in poly(benzimidazole imide)s and improvement in H<sub>2</sub>O-absorption and transparency†

Guangtao Qian, Fengna Dai, Haiquan Chen, Mengxia Wang, Mengjie Hu,  
Chunhai Chen and Youhai Yu \*

5-Amine-2-(4-amino-benzene)-1-phenyl-benzimidazole (*N*-PhPABZ) was successfully synthesized and polymerized with 3,3',4,4'-biphenyl tetracarboxylic dianhydride (BPDA) to obtain a novel *N*-phenyl-poly(benzimidazole imide) (*N*-Ph-PBII). The successful incorporation of *N*-phenyl addressed the issue of high H<sub>2</sub>O-absorption of traditional PBIs while retained the superheat resistance property. The resulting *N*-Ph-PBII possessed a high glass-transition temperature ( $T_g$ ) up to 425 °C and a low affinity for water of 1.4%. Furthermore, the loose molecular packing and noncoplanar structures led to an increase in optical transparency for the modified PBII.

## 1. Introduction

Poly(benzimidazole imide) (PBIs), combining the superiority of polyimides (PIs) and polybenzimidazoles (PBIs), are a class of promising polymers in engineering and science.<sup>1–3</sup> Among their outstanding properties, the high thermal properties with  $T_g$  values normally greater than 400 °C have gained attention.<sup>4,5</sup> Previous research has proven that the excellent superheat-resistant ability of PBIs can be ascribed to the intermolecular hydrogen bonds formed between the proton donors (N–H group) and proton acceptors (–N= or C=O).<sup>6,7</sup> Also, the benzimidazole (BI)-containing diamines strengthen the charge transfer (CT) interaction between the molecular chains with their higher electron-donating properties, facilitating the increased  $T_g$  value of polymers.<sup>8,9</sup>

As a key additive, heteroaromatic BI ring plays a critical role for the improving thermal properties of PBIs. However, the N–H in the key unit leads to an increased chance for hydrogen-bonded water molecules formation, resulting polymers with a high affinity of water.<sup>10,11</sup> For instance, the water absorption ( $W_A$ ) can reach 15–18 wt% for poly(2,2'-*m*-(phenylene)-5,5'-bibenzimidazole) (PBI) and 6–7 wt% for the PBIs derived from 5(6)-amino-2-(4-aminobenzene)-benzimidazole (PABZ) and BPDA.<sup>12,13</sup> Among them, the traditional PBIs can be used as a candidate material for flexible substrates in various image display devices; however, their high  $W_A$  may lead the package cracking, degradation of

dielectric properties, and failures of the adhesion to metal, restricting the application.<sup>13,14</sup> Hence, low H<sub>2</sub>O-absorption PBIs without compromising their superior properties are desirable.

Our previous study showed that, having appropriate *N*-substituents, such as *N*-methyl, in the BI ring can solve the problem of high  $W_A$  in PBIs.<sup>14</sup> However, this series of *N*-methyl-PBIs have relatively lower  $T_g$  values because of the hindrance of intermolecular H-bonding formation. Recent researches have proved that the incorporation of large rigid side-bases can enhance thermal properties of polymers through their steric hindrance.<sup>15,16</sup> So *N*-PhPABZ with a bulk *N*-phenyl-substituent was designed and synthesized (Scheme 1) in this work, which may provide PBIs with low  $W_A$  and high  $T_g$ . *N*-PhPABZ-BPDA was successfully prepared (Scheme 2) and its physical properties was compared with that of the traditional PBII (PABZ-BPDA).

## 2. Experiment

### 2.1 Materials

2,4-Dinitrofluorobenzene, aniline and 4-nitrobenzoyl chloride were purchased from Shanghai Haohong Biomedical Technology Co. Ltd. and Aladdin Chemical Co. Ltd., respectively. Other chemicals used in this study were purchased from Sino-pharm Chemical Reagent Beijing Co. Ltd. Among them, BPDA were dried overnight at 80 °C under vacuum, and *N,N*-dimethylacetamide (DMAc) were purified by vacuum distillation, prior to use. All the other commercially available reagents were used without further purification.

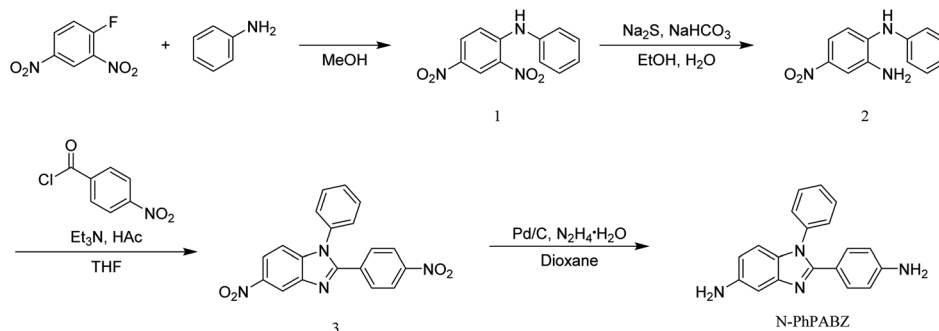
### 2.2 Characterization

<sup>1</sup>H NMR and <sup>1</sup>H–<sup>1</sup>H COSY data were recorded on a Bruker 600 AVANCE III spectrometer, using dimethyl sulfoxide-*d*<sub>6</sub> as

Center for Advanced Low-Dimension Materials, State Key Laboratory for Modification of Chemical Fibers and Polymer Materials, College of Material Science and Engineering, Donghua University, Shanghai 201620, P. R. China. E-mail: yuyouhai@dhu.edu.cn

† Electronic supplementary information (ESI) available. See DOI: 10.1039/d0ra10138a



Scheme 1 Synthesis of *N*-PhPABZ.

a solvent. Elemental analyses were determined in by Elmentar Vario EL-III. The inherent viscosities ( $\eta_{\text{inhs}}$ ) were measured with an Ubbelohde viscometer at  $25 \pm 0.1$  °C with a concentration of  $0.5 \text{ g L}^{-1}$  in DMAc. Attenuated total reflectance Fourier transform infrared (ATR-FTIR) spectra were measured at a Nicolet 6700 infrared spectrometer in the range of  $4000\text{--}700 \text{ cm}^{-1}$ . UV-vis spectra were recorded on a Shimadzu UV-3600 spectrophotometer in a transmittance mode with the wavelength range of  $300\text{--}700 \text{ cm}^{-1}$ . Wide-angle X-ray diffraction (WAXD) was collected on a Rigaku Denki D/MAX-2500 diffractometer at room temperature. The thermogravimetric analysis was assessed using Discovery TGA 550 with a constant heating rate of  $10 \text{ }^\circ\text{C min}^{-1}$  under nitrogen. Dynamic mechanical analysis (DMA) was performed on a TA Instrument DMA Q800 in a tension mode with a heating rate of  $5 \text{ }^\circ\text{C min}^{-1}$  and a frequency of 1 Hz. Coefficient of thermal expansion (CTE) was examined using a TA Instrument TMA Q400 in the range of  $50\text{--}300$  °C at a heating rate of  $5 \text{ }^\circ\text{C min}^{-1}$  with a fixed load of  $0.5 \text{ g } \mu\text{m}^{-1}$  (film thickness) in nitrogen. The tensile properties of polymer films were evaluated on a Shimadzu AG-I universal testing apparatus at speed of  $5.0 \text{ mm min}^{-1}$ , and tensile strength ( $\sigma$ ), tensile modulus ( $E$ ) and elongation at break ( $\epsilon$ ) were demonstrated as the average of five strips. The net charge on nitrogen atoms and energy minimized structures on the molecules was achieved through the B3LYP (Becke, three-parameter, Lee–Yang–Parr) exchange–correlation functional for the 6-311G(d,p) basis set basis set in Gaussian 09W.

$W_A$  of the polymer films was measured by dipping in distilled water. In detail, large film specimens ( $>0.1 \text{ g}$ ) were weighed before being immersed in water at  $25$  °C for 24 h and then blotted carefully clean with tissue paper and weighed. The water absorption ratio was calculated from the follow equation:

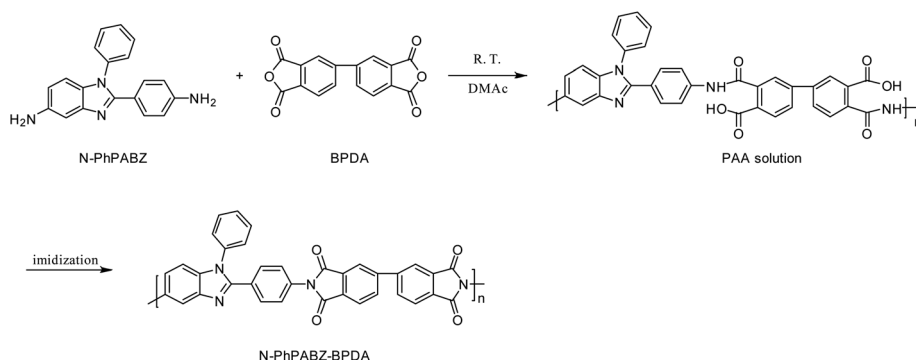
$$W_A = [(W_{\text{wet}} - W_{\text{dry}})/W_{\text{dry}}] \times 100\%.$$

Among them  $W_{\text{dry}}$  is the initial weight of the samples,  $W_{\text{wet}}$  is the sample weight after treatment and  $W_A$  is the mean value of three parallel samples.

### 2.3 Synthesis of monomers

**2.3.1 2,4-Dinitrodiphenylamine (1).** Aniline (5.0 g, 53.7 mmol) was added into a stirred mixture of 2,4-dinitrofluorobenzene (9.5 g, 51.1 mmol) in methanol (100.0 mL) maintained at  $0$  °C. The mixture was stirred at room temperature for 18 h (TLC monitoring) and then filtrated. The residue was dried in vacuum at  $80$  °C for 24 h to afford the title compound (11.3 g, yield: 85.3%) which was used for the next reaction without purification. Melting point:  $160$  °C.  $^1\text{H NMR}$  (DMSO- $d_6$ , ppm):  $\delta = 10.16$  (s, 1H), 8.90 (d, 1H,  $J = 2.7$  Hz), 8.23 (dd, 1H,  $J = 9.6$  Hz, 2.8 Hz), 7.57–7.49 (m, 2H), 7.44–7.32 (m, 3H), 7.10 (d, 1H,  $J = 9.5$  Hz). Anal. calcd for  $\text{C}_{12}\text{H}_9\text{N}_3\text{O}_4$ : C, 55.60; H, 3.50; N, 16.21. Found: C, 55.21; H, 3.82; N, 16.22.

**2.3.2 4-Nitro-1-*N*-phenylbenzene-1,2-diamine (2).** To a solution of compound 1 (10.0 g, 38.6 mmol) in the solvent

Scheme 2 Reaction schemes of *N*-PhPABZ-BPDA.

system ethanol (80.0 mL)-water (40 mL) was added sodium bicarbonate (3.9 g, 46.3 mmol) and sodium sulfide (3.6 g, 46.3 mmol). The reaction was allowed to warm to 80 °C and stirred overnight. After this time, the reaction was cooled with an ice-water bath and then poured into water. The precipitate which appeared was collected using suction filtration and dried to yield compound 2 as a brown colored powder (7.2 g, yield: 81.8%). Melting point: 123 °C.  $^1\text{H}$  NMR (DMSO- $d_6$ , ppm):  $\delta$  = 7.79 (s, 1H), 7.58 (d, 1H,  $J$  = 2.7 Hz), 7.46 (dd, 1H,  $J$  = 8.9 Hz, 2.7 Hz), 7.34 (t, 2H,  $J$  = 7.8 Hz), 7.16 (d, 2H,  $J$  = 7.9 Hz), 7.07 (d, 1H,  $J$  = 8.9 Hz), 7.01 (t, 1H,  $J$  = 7.3 Hz), 5.44 (s, 2H). Anal. calcd for  $\text{C}_{12}\text{H}_{11}\text{N}_3\text{O}_2$ : C, 62.87; H, 4.84; N, 13.91. Found: C, 63.11; H, 4.81; N, 14.12.

**2.3.3 5-Nitro-2-(4-nitrobenzene)-1-phenyl-benzimidazole (3).** To compound 2 (5.0 g, 21.8 mmol) and triethylamine (2.6 g, 26.2 mmol) in tetrahydrofuran (50.0 mL) at 0 °C was added 4-nitrobenzoyl chloride (4.9 g, 26.2 mmol) in equal portions over 0.5 h. The reaction was allowed to stir at room temperature for 16 h. Water (100.0 mL) was added and the reaction mixture was filtered. After drying, the residue was dissolved in the acetic acid (200.0 mL) and the solution was heated under argon at 120 °C for 3 h. The mixture was then diluted with water and filtered thru filtration fabric (ethanol rinse). The residue purified by recrystallization from DMSO yielded compound 3 (7.0 g, yield: 89.3%) as a yellow powder. Melting point: 195 °C.  $^1\text{H}$  NMR (DMSO- $d_6$ , ppm):  $\delta$  = 7.50 (dd, 1H,  $J$  = 8.6 Hz, 2.1 Hz), 7.10 (d, 1H,  $J$  = 1.6 Hz), 6.56 (d, 1H,  $J$  = 8.6 Hz), 6.15 (s, 2H), 5.23 (d, 1H,  $J$  = 4.4 Hz), 2.79 (d, 3H,  $J$  = 4.7 Hz). Anal. calcd for  $\text{C}_{19}\text{H}_{12}\text{N}_4\text{O}_4$ : C, 63.33; H, 3.36; N, 15.55. Found: C, 63.35; H, 3.65; N, 15.29.

**2.3.4 5-Amine-2-(4-aminobenzene)-1-phenyl-benzimidazol (N-PhPABZ).** Compound 3 (5.0 g, 13.8 mmol) and palladium catalyst (10% Pd/C, 0.5 g) was dissolved in methanol (50.0 mL). After stirred for a further 1 h whilst being refluxed, the mixture was hydrogenated by the dropwise addition of 7.0 mL of hydrazine hydrate. The reaction was refluxed for 4.5 hours and then cooled to room temperature. The catalyst was removed by filtration, and then the filtrate was poured into water (100.0 mL). The precipitate was filtered off and purified in water/EtOH to afford the desired compound (a white powder, 3.8 g, yield: 92.8%). Melting point: 270 °C.  $^1\text{H}$  NMR (DMSO- $d_6$ , ppm):  $\delta$  = 7.50 (dt, 3H,  $J$  = 27.1 Hz, 7.3 Hz), 7.31 (d, 2H,  $J$  = 7.4 Hz), 7.12 (d, 2H,  $J$  = 8.6 Hz), 6.81 (dd, 2H,  $J$  = 11.0 Hz, 5.1 Hz), 6.52 (dd, 1H,  $J$  = 8.5 Hz, 1.9 Hz), 6.43 (d, 2H,  $J$  = 8.6 Hz), 5.44 (s, 2H), 4.79 (s, 2H). Anal. calcd for  $\text{C}_{19}\text{H}_{16}\text{N}_4$ : C, 75.98; H, 5.37; N, 18.65. Found: C, 75.60; H, 5.65; N, 18.88.

## 2.4 Preparation of the N-PhPABZ-BPDA film

**N-PhPABZ-BPDA** was prepared through a typical two-stage thermal imidization (Scheme 2). In detail, a sealed bottle charged with anhydrous DMAc (9.5 mL), **N-PhPABZ** (1.2015 g, 4.0 mmol) was mixed in. After the diamine was completely dissolved, **BPDA** (1.1768 g, 4.0 mmol) was added slowly at a rate sufficient to maintain the reaction solution clear (addition time *ca.* 2.0 h). The mixture was continuously stirred under room temperature for 24 h. The above solution was then cast on a dust-free glass disc, and the glass plate was placed in an oven

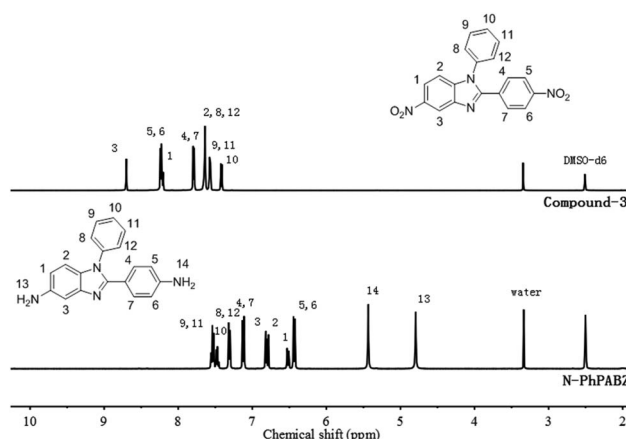


Fig. 1  $^1\text{H}$  NMR spectra of synthesized monomers (compound 3 and N-PhPABZ).

at 80 °C overnight to slowly evaporate the solvent. Subsequently, the polyamic acid (PAA) film was heated at 200 °C, 300 °C, and 400 °C each for 1 h to complete the imidization process. Finally, the glass disc was cooled to room temperature and soaked in deionized water to get the desired PBII film.

## 2.5 Other monomers and PABZ-BPDA

The synthesis processes of PABZ and **PABZ-BPDA** had been illustrated in our previous study.<sup>14</sup> In this work, the physical properties of the traditional PBII (**PABZ-BPDA**) were used as references.

# 3. Results and discussion

## 3.1 Molecular structure

As shown in Scheme 1, the N-Ph was successfully introduced in **N-PhPABZ** as a key unit through the use of aniline with the above reaction sequence. The new BI-diamine was fully characterized by means of elemental analysis, FTIR spectrum,  $^1\text{H}$  NMR (Fig. 1) and  $^1\text{H}$ - $^1\text{H}$  COSY (Fig. 2) spectra. In the  $^1\text{H}$  NMR spectra of **N-PhPABZ**, no signal (*ca.* 11.84 ppm) of the -NH-

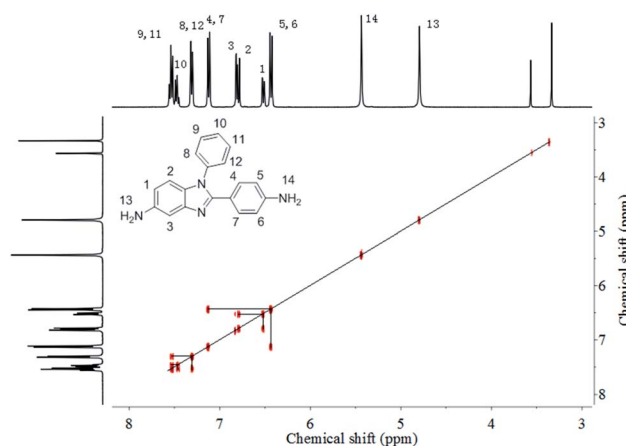


Fig. 2  $^1\text{H}$ - $^1\text{H}$  COSY spectrum of N-PhPABZ.



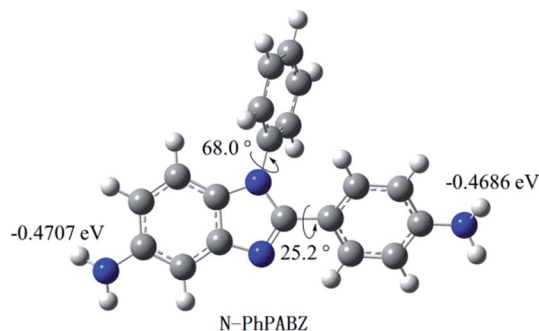


Fig. 3 Energy minimized structure of *N*-PhPABZ and net charges on the nitrogen atoms of amino groups calculated by the DFT [B3LYP/6-311G(d,p)] calculations.

proton in the BI group was observed, and three sets of peaks (7.5–7.3 ppm) were attributed to aromatic protons, proving the placement of phenyl on BI nitrogen atom. To further assign the aromatic protons of *N*-Ph in the diamine,  $^1\text{H}$ - $^1\text{H}$  COSY spectra had been given and the data accorded with the expected structure. In addition, the high field peak at 5.44 ppm (H-14) and 4.79 ppm (H-13) would correspond to the amine protons linked to phenyl ring and BI unit. The electron-donating effect of BI on amine H-13 caused an obviously 0.65 ppm high-field shift in comparison with H-14 attached to phenyl ring, that is, the terminal amine attached to BI ring had higher

nucleophilicity and reactivity than the phenyl linked  $-\text{NH}_2$ . It indicated that the employ of *N*-Ph did not affect the nucleophilic advantage for such diamines.

To get clear geometric optimization conformation, the energy minimized structure of *N*-PhPABZ was calculated by the DFT [B3LYP/6-311G(d,p)] method, using the Gaussian 09W software (Fig. 3). Obviously, the net charge of the amine N atoms on BI ring was significantly higher than that on phenyl ring, because of the higher electron-donating property of BI group. Since the nucleophilicity of diamines increased by introducing strong electron-donating BI, it could be inferred that *N*-PhPABZ would possess higher nucleophilicity than full-phenyl diamines. Furthermore, the stable geometry proved the resultant diamine possessed more noncoplanar conformation in comparison with PABZ. As depicted in FOHURE 3, the dihedral angle between phenyl ring and imide ring exhibited  $25.2^\circ$ . It was indicative of the BI-diamine molecular structure was significantly affected by the *N*-substitution group, and its steric hindrance resulted in the distorted backbone.

### 3.2 Polymer characteristics

ATR-FTIR was utilized to investigate the molecule structures of the PI film as shown in Fig. 4A. The typical characteristic imide peak at around 1783, 1719,  $1367\text{ cm}^{-1}$  were assigned to imide carbonyl asymmetric stretching, imide carbonyl symmetric stretching and cyclic C–N stretching, respectively, and the peaks corresponding to the C=O in  $-\text{CONH}-$  ( $1660\text{ cm}^{-1}$ , gray band

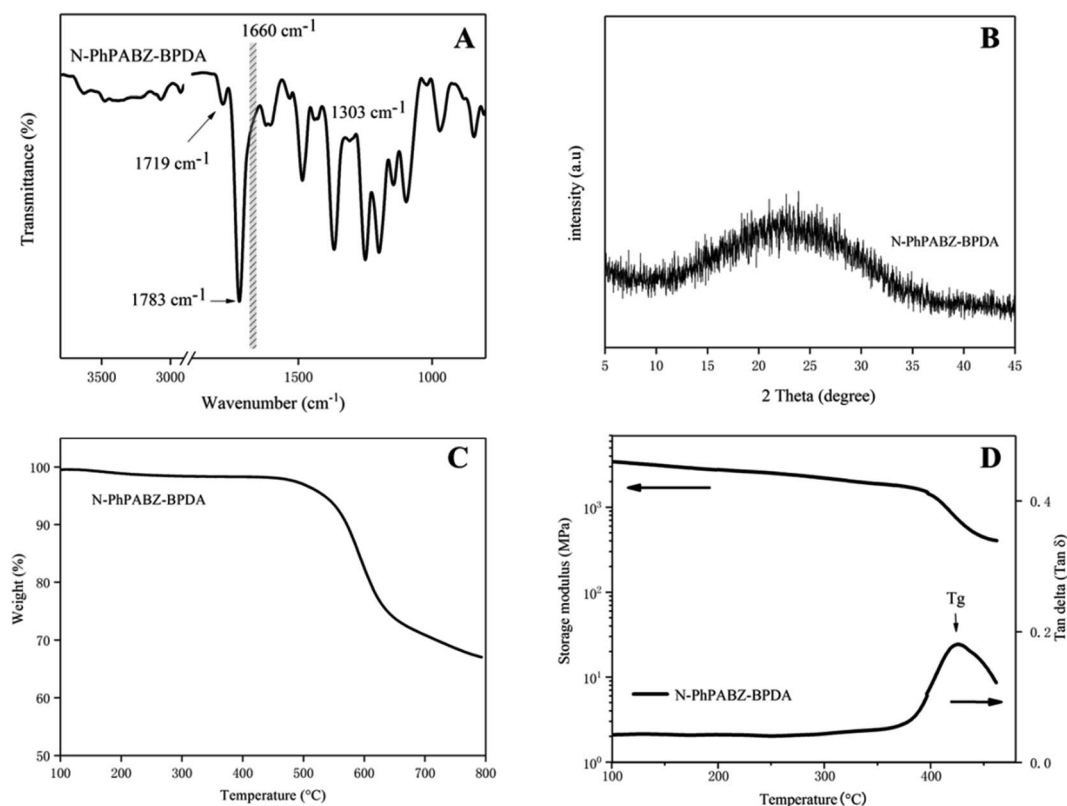


Fig. 4 ATR-FTIR spectra (A), WAXD diffractogram (B), TGA thermogram (C) and DMA curve (D) of *N*-PhPABZ-BPDA.





Table 1 Properties of the PBII films

Sample no.	$\eta_{inh}$ (PAA) (dL g <sup>-1</sup> )	$T_g^a$ (DMA) (°C)	$T_d^{5b}$ (N <sub>2</sub> ) (°C)	$\sigma$ (MPa)	$E$ (GPa)	$\epsilon$ (%)	CTE <sup>c</sup> (ppm K <sup>-1</sup> )	$W_A$ (%)
<b>PABZ-BPDA</b>	1.16 <sup>d</sup>	423 <sup>d</sup>	549 <sup>d</sup>	218 <sup>d</sup>	6.7 <sup>d</sup>	5.9 <sup>d</sup>	11 <sup>d</sup>	5.9 <sup>d</sup>
<b>N-PhPABZ-BPDA</b>	0.81	425	534	130	4.7	3.7	27	1.4

<sup>a</sup> Glass transition temperature was recorded by DMA. <sup>b</sup> 5% weight loss temperature was recorded by TGA. <sup>c</sup> Coefficient of thermal expansion along the X-Y direction, measured in the range of 100–200 °C with TMA. <sup>d</sup> Data from ref. 14.

domain) was hardly observed, clarifying the imidization process was fully completed.<sup>17,18</sup> Moreover, the characteristic absorption of BI ring at 1303 cm<sup>-1</sup> (imidazole ring breathing peak) confirmed the successful incorporation of the characteristic group.<sup>19,20</sup> Additionally, the characteristic absorption peaks of imide C=O in the **N-PhPABZ** agreed well with the values of free carbonyl, that was no hydrogen bonding occurred in the prepared PBII.<sup>14</sup> The results implied the *N*-Ph on the imidazole nitrogen atoms limited the formation of intermolecular H-bonding and increased the difficulty in the hydrogen-bonded water molecules formation.

The chain aggregation conducted by X-ray diffraction measurement was illustrated in Fig. 4B. The **N-PhPABZ-BPDA** film exhibited a broad diffraction peak centered at  $2\theta = 22.5^\circ$ , typical of an amorphous material. The loose molecular packing was attributed to the increased interchain distances resulted from the existence of the bulky *N*-phenyl in the backbone. In contrast, the reported PBIIIs usually had highly ordered molecular arrangements and close chain packing with their H-bonding, which could provide materials with deep color because of the enhanced charge-transfer (CT) interactions.<sup>4,7,21</sup> In this work, with the incorporation of *N*-substituent, the density and packing coefficient decreased, and the optical transparency of the PBII might be improved.

**3.2.1 Physical properties of N-PhPABZ-BPDA.** The thermal properties of **N-PhPABZ-BPDA** were evaluated by TGA (Fig. 4C), DMA (Fig. 4D) and TMA (Fig. S1†), and the analysis data was presented in Table 1. The 5% weight loss temperature was above 500 °C, which is similar to that of **PABZ-BPDA**, testifying **N-PhPABZ-BPDA** retained the advantages of traditional PBII in higher thermal stability. In general, the more conjugated rigid chain led to a higher thermal stability for PIs.<sup>22,23</sup> This was because the resulting  $\pi$ -electron system facilitated rapid heat transfer between molecular bonds, which prevented the rupture of polymer main chains when they experience a high temperature. The rigidity of imidazole diamine had not decreased after the introduction of rigid *N*-Ph, thus, **N-PhPABZ-BPDA** possessed a high thermal decomposition temperature.

In Fig. 4D, the peak temperature of the tan delta curve was regarded as  $T_g$  value,<sup>24</sup> and the value of **N-PhPABZ-BPDA** was almost the same as that of **PABZ-BPDA**, which was up to 425 °C. In previous studies, the outstanding  $T_g$  of PBIIIs could be explained from two aspects. First, the intermolecular H-bonding (C=N $\cdots$ N-H and C=O $\cdots$ N-H) derived from imidazole unit restricted chain-segment motion. Second, the higher nucleophilic of BI-contained diamines resulted in an increased

CT interaction and the strengthened physical interaction between the molecular chains also increased the difficulty in molecular-chain motion when these PBIIIs experienced a high temperature.<sup>6–9</sup> In this work, **N-PhPABZ**, as a modified BI-diamine, inherited the superiority of higher nucleophilicity, evidenced by the <sup>1</sup>H NMR and calculation results. Furthermore, the rigid *N*-Ph group limited the rotational freedom around backbone of PIs. As expected, The **N-PhPABZ-BPDA** film displayed a high  $T_g$ .

It was believed that the CTE values were susceptible to the alteration in molecular-chain orientation, and the interchain interaction and chain stiffness/linearity played an key role in the occurrence of in-plane orientation.<sup>25,26</sup> The **PABZ-BPDA** had a high level of coplanarity and much H-bonding, which was benefit to the spontaneous orientation during thermal imidization, therefore, such series of PIs exhibited higher dimensional stability and lower CTE. Indeed, with a bulky pendant group and distorted conformations, **N-PhPABZ-BPDA** had relatively higher CTE compared with the **PABZ-BPDA**. However, the CTE value of 27 ppm K<sup>-1</sup> was close to that of the commercially available Kapton H (Dupont) used as a representative heat-resisting high polymer.<sup>27</sup>

As the result (Table 1 and Fig. S2†), **N-PhPABZ-BPDA** had a tensile strength of 130.0 MPa, a modulus of 4.7 GPa and an elongation at break of 3.7%, affirming its toughness and flexibility. It was believed that PI with higher crystallinity and

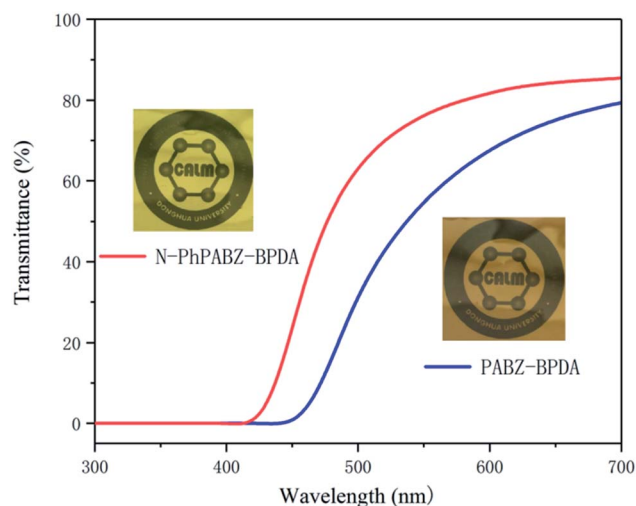


Fig. 5 UV-vis spectra and images of the PBII films.



Table 2 Optical properties of the PBII films

Sample no.	Thickness ( $\mu\text{m}$ )	$\lambda_{\text{cut-off}}^a$ (nm)	$T_{500}^b$ (%)
PABZ-BPDA	20	436	31
N-PhPABZ-BPDA	21	405	63

<sup>a</sup> Cutoff wavelength, the wavelength with a transmittance of lower than 1%. <sup>b</sup> Transmittance at 500 nm.

intermolecular interactions possessed higher mechanical properties.<sup>28</sup> The obviously decreasing mechanical performance of the N-Ph-PBII had been observed in the Table 1. Based on the above analysis, the higher mechanical properties of PABZ-BPDA resulted from its semi-crystalline state, and the lower properties of PABZ-BPDA corresponded to its amorphous state. Besides, the presence of N-substituent bulky not only hindered hydrogen bond formation but also loosened the chain packing, resulting the reduced physical interaction and the decreasing trend of  $T_g$ . Nevertheless, the tensile strength exceeded 100 MPa, the initial modulus was over 2 GPa, which was able to meet the requirements in commercial use.<sup>29,30</sup>

Polymers containing imidazole rings usually had a high affinity for water. The primary cause was the hydrophilic imidazole N-H group which could form hydrogen bonds with water. So the feasible substituents on the imidazole nitrogen atom could hinder the hydrogen-bonded water molecules formation, partially eliminating the issue of high H<sub>2</sub>O-absorption for such polymers. Obviously, N-PhPABZ-BPDA illustrated a low H<sub>2</sub>O-absorption down to 1.4%, and the value decreased 76% compared to that of PABZ-BPDA (Table 1). It verified that the introduction of N-Ph was one of the useful technologies for healing the inherent problem of high  $W_A$  for the PBII series.

The cut-off wavelength values and transmittances at 500 nm of the N-Ph-PBII film were listed in Fig. 5 and Table 2, which was investigated by UV-vis spectroscopy. The color intensity of PIs was generally related to the charge transfer complex (CTC) formation theory.<sup>31,32</sup> According to the theory, the intra- and inter-molecular CTC formation was easily affected by electron-accepting property of dianhydride, electron-donating property of diamine and stacking state of chain-segments. Polyimides with bulky electron withdrawing units, flexible groups or non-coplanar structures possessed lighter color compared with PIs had a rigid chain. PABZ, as one of traditional BI-diamines, had a strong electron-donating ability and a stiff framework, and thus PABZ-BPDA presented a deep color. N-PhPABZ also showed strong nucleophilicity, however, its N-Ph moiety had the ability to distort molecules and increased the spacing between backbones for the polymers contained it. As a result, the N-PhPABZ-PBII had a superior optical transparency than that derived from PABZ.

## 4. Conclusions

A novel N-phenyl-poly(benzimidazole imide) (N-Ph-PBII) had been prepared by polymerization of BPDA and a bulk N-phenyl-

substituted PABZ. The N-substituent hindered the hydrogen-bonded water molecules formation and the N-Ph-PBII showed lower  $W_A$ . Furthermore, the merged N-Ph distorted the backbone and increased the difficulty of chain motion in the prepared PIs. As a result, the N-PhPABZ-BPDA film exhibited an extremely high  $T_g$  and significantly improved optical transparency. Although the dimensional stability and mechanical properties of the N-Ph-PBII were lower than traditional PBIIs, but they could still meet the demand for practical application. This study provided new insights to prepare the modified PBIIs with desirable properties.

## Conflicts of interest

There are no conflicts to declare.

## References

- Y. Jiao, G. Chen, H. Zhou, F. Zhang and X. Chen, *J. Polym. Res.*, 2019, **26**, 1–12.
- S. Yuan, X. Guo, D. Aili, C. Pan, Q. Li and J. Fang, *J. Membr. Sci.*, 2014, **454**, 351–358.
- Y. Tian, L. Luo, Q. Yang, L. Zhang, M. Wang, D. Wu, X. Wang and X. Liu, *Polymer*, 2020, **188**, 122100.
- S. Wang, H. Zhou, G. Dang and C. Chen, *J. Polym. Sci., Part A: Polym. Chem.*, 2009, **47**, 2024–2031.
- J. Liu, Q. Zhang, Q. Xia, J. Dong and Q. Xu, *Polym. Degrad. Stab.*, 2012, **97**, 987–994.
- Y. Zhuang, X. Liu and Y. Gu, *Polym. Chem.*, 2012, **3**, 1517–1525.
- L. Luo, J. Yao, X. Wang, K. Li, J. Huang, B. Li and X. Liu, *Polymer*, 2014, **55**, 4258–4269.
- M. Lian, X. Lu and Q. Lu, *Macromolecules*, 2018, **51**, 10127–10135.
- L. Luo, Y. Dai, Y. Yuan, X. Wang and X. Liu, *Macromol. Rapid Commun.*, 2017, **38**, 1700404.
- D. W. Tomlin, A. V. Fratini, M. Hunsaker and W. W. Adams, *Polymer*, 2000, **41**, 9003.
- G. Qian, H. Chen, G. Song, J. Yao, M. Hu and C. Chen, *J. Polym. Sci., Part A: Polym. Chem.*, 2020, **58**, 969–976.
- T. S. Chung, *J. Macromol. Sci., Rev. Macromol. Chem. Phys.*, 1997, **37**, 277–301.
- M. Hasegawa, Y. Hoshino, N. Katsura and J. Ishii, *Polymer*, 2017, **111**, 91–102.
- G. Qian, H. Chen, G. Song, F. Dai and J. Yao, *Polymer*, 2020, **196**, 122482.
- Z. Sun, M. Liu, L. Yi and Y. Wang, *RSC Adv.*, 2013, **3**, 7271–7276.
- H. Choi, I. S. Chung, K. Hong, C. E. Park and S. Y. Kim, *Polymer*, 2008, **49**, 2644–2649.
- Y. K. Xu, M. S. Zhan and K. Wang, *J. Polym. Sci., Part B: Polym. Phys.*, 2004, **42**, 2490–2501.
- S. Diaham, M. L. Locatelli, T. Lebey and D. Malec, *Thin Solid Films*, 2011, **519**, 1851–1856.
- P. Musto, F. E. Karasz and W. J. MacKnight, *Polymer*, 1993, **34**, 2934–2945.



- 20 S. Qing, W. Huang and D. Yan, *J. Polym. Sci., Part A: Polym. Chem.*, 2005, **43**, 4363–4372.
- 21 G. Song, X. Zhang, D. Wang, X. Zhao, H. Zhou and C. Chen, *Polymer*, 2014, **55**, 3242–3246.
- 22 Y. N. Sazanov, F. S. Florinsky and M. M. Koton, *Eur. Polym. J.*, 1979, **15**, 781–786.
- 23 K. P. Pramoda, T. S. Chung and S. L. Liu, *Polym. Degrad. Stab.*, 2000, **67**, 365–374.
- 24 O. Acar, *Polym. Test.*, 2019, **77**, 105883.
- 25 M. Hasegawa, K. Okuda, M. Horimoto, Y. Shindo, R. Yokota and M. Kochi, *Macromolecules*, 1997, **30**, 5745–5752.
- 26 J. H. Jou, P. T. Huang, H. C. Chen and C. N. Liao, *Polymer*, 1992, **33**, 967–974.
- 27 C. E. Sroog, *Prog. Polym. Sci.*, 1991, **16**, 561–694.
- 28 L. Luo, J. Zhang, J. Huang, Y. Feng, C. Peng, X. Wang and X. Liu, *J. Appl. Polym. Sci.*, 2016, **133**, 44000.
- 29 Y. Zhuang, J. G. Seong, Y. S. Do, H. J. Jo, M. J. Lee and G. Wang, *Macromolecules*, 2014, **47**, 7947–7957.
- 30 R. Sulub-Sulub, M. I. Loria-Bastarrachea, H. Vázquez-Torres, J. L. Santiago-García and M. Aguilar-Vega, *J. Membr. Sci.*, 2018, **563**, 134–141.
- 31 R. S. Mulliken, *J. Am. Chem. Soc.*, 1952, **74**, 811.
- 32 M. Hasegawa and K. Horie, *Prog. Polym. Sci.*, 2001, **26**, 259–335.

